

- Estornes Y, Toscano F, Virard F et al (2012) dsRNA induces apoptosis through an atypical death complex associating TLR3 to caspase-8. *Cell Death Differ* 19:1482–1494
- Ferreon JC, Ferreon AC, Li K et al (2005) Molecular determinants of TRIF proteolysis mediated by the hepatitis C virus NS3/4A protease. *J Biol Chem* 280:20483–20492
- Florentin J, Aouar B, Dental C et al (2012) HCV glycoprotein E2 is a novel BDCA2 ligand and acts as an inhibitor of IFN production by plasmacytoid dendritic cells. *Blood* 120:4544–4551
- Gack MU, Shin YC, Joo CH et al (2007) TRIM25 RING-finger E3 ubiquitin ligase is essential for RIG-I-mediated antiviral activity. *Nature* 446:916–920
- Harada K, Sato Y, Itatsu K et al (2007) Innate immune response to double-stranded RNA in biliary epithelial cells is associated with the pathogenesis of biliary atresia. *Hepatology* 46:1146–1154
- He S, Wang L, Miao L et al (2009) Receptor interacting protein kinase-3 determines cellular necrotic response to TNF- α . *Cell* 137:1100–1111
- He S, Liang Y, Shao F et al (2011) Toll-like receptors activate programmed necrosis in macrophages through a receptor-interacting kinase-3-mediated pathway. *Proc Natl Acad Sci USA* 108:20054–20059
- Hogbom M, Collins R, van den Berg S et al (2007) Crystal structure of conserved domains 1 and 2 of the human DEAD-box helicase DDX3X in complex with the mononucleotide AMP. *J Mol Biol* 372:150–159
- Horner SM, Liu HM, Park HS et al (2011) Mitochondrial-associated endoplasmic reticulum membranes (MAM) form innate immune synapses and are targeted by hepatitis C virus. *Proc Natl Acad Sci USA* 108:14590–14595
- Jelinek I, Leonard JN, Price GE et al (2011) TLR3-specific double-stranded RNA oligonucleotide adjuvants induce dendritic cell cross-presentation, CTL responses, and antiviral protection. *J Immunol* 186:2422–2429
- Jin B, Wang RY, Qiu Q et al (2007) Induction of potent cellular immune response in mice by hepatitis C virus NS3 protein with double-stranded RNA. *Immunology* 122:15–27
- Kanda T, Steele R, Ray R et al (2009) Inhibition of intrahepatic gamma interferon production by hepatitis C virus nonstructural protein 5A in transgenic mice. *J Virol* 83:8463–8469
- Kawai T, Akira S (2009) The roles of TLRs, RLRs and NLRs in pathogen recognition. *Int Immunol* 21:317–337
- Khvalevsky E, Rivkin L, Rachmilewitz J et al (2007) TLR3 signaling in a hepatoma cell line is skewed towards apoptosis. *J Cell Biochem* 100:1301–1312
- Kim YS, Lee SG, Park SH et al (2001) Gene structure of the human DDX3 and chromosome mapping of its related sequences. *Mol Cells* 12:209–214
- Kono H, Rock KL (2008) How dying cells alert the immune system to danger. *Nat Rev Immunol* 8:279–289
- Larrubia JR, Benito-Martinez S, Calvino M et al (2008) Role of chemokines and their receptors in viral persistence and liver damage during chronic hepatitis C virus infection. *World J Gastroenterol* 14:7149–7159
- Li K, Foy E, Ferreon JC et al (2005a) Immune evasion by hepatitis C virus NS3/4A protease-mediated cleavage of the Toll-like receptor 3 adaptor protein TRIF. *Proc Natl Acad Sci USA* 102:2992–2997
- Li XD, Sun L, Seth RB et al (2005b) Hepatitis C virus protease NS3/4A cleaves mitochondrial antiviral signaling protein off the mitochondria to evade innate immunity. *Proc Natl Acad Sci USA* 102:17717–17722
- Li K, Li NL, Wei D et al (2012) Activation of chemokine and inflammatory cytokine response in hepatitis C virus-infected hepatocytes depends on Toll-like receptor 3 sensing of hepatitis C virus double-stranded RNA intermediates. *Hepatology* 55:666–675
- Lim EJ, Chin R, Angus PW et al (2012) Enhanced apoptosis in post-liver transplant hepatitis C: effects of virus and immunosuppressants. *World J Gastroenterol* 18:2172–2179
- Lindenbach BD, Thiel HJ, Rice CM (2007) Flaviviridae: the viruses and their replication. In: Knipe DM, Howley PM (eds) *Fields virology*. Lippincott Williams & Wilkins, Philadelphia, pp 1117–1118
- Liu HM, Loo YM, Horner SM et al (2012) The mitochondrial targeting chaperone 14–3-3 ϵ regulates a RIG-I translocon that mediates membrane association and innate antiviral immunity. *Cell Host Microbe* 11:528–537
- Longhi MP, Trumppfeller C, Idoyaga J et al (2009) Dendritic cells require a systemic type I interferon response to mature and induce CD4⁺ Th1 immunity with poly I:C as adjuvant. *J Exp Med* 206:1589–1602
- Loo YM, Owen DM, Li K et al (2006) Viral and therapeutic control of IFN- β promoter stimulator 1 during hepatitis C virus infection. *Proc Natl Acad Sci USA* 103:6001–6006
- Lucas M, Schachterle W, Oberle K et al (2007) Dendritic cells prime natural killer cells by trans-presenting interleukin 15. *Immunity* 26:503–517
- Matsumoto M, Seya T (2008) TLR3: interferon induction by double-stranded RNA including poly(I:C). *Adv Drug Deliv Rev* 60:805–812
- Matsumoto M, Oshiumi H, Seya T (2011) Antiviral responses induced by the TLR3 pathway. *Rev Med Virol*. doi:10.1002/rmv.680
- McCartney S, Vermi W, Gilfillan S et al (2009) Distinct and complementary functions of MDA5 and TLR3 in poly(I:C)-mediated activation of mouse NK cells. *J Exp Med* 206:2967–2976
- McLauchlan J, Lemberg MK, Hope G et al (2002) Intramembrane proteolysis promotes trafficking of hepatitis C virus core protein to lipid droplets. *EMBO J* 21:3980–3988
- Meylan E, Burns K, Hofmann K et al (2004) RIP1 is an essential mediator of Toll-like receptor 3-induced NF- κ B activation. *Nat Immunol* 5:503–507
- Morosky SA, Zhu J, Mukherjee A et al (2011) Retinoic acid-induced gene-1 (RIG-I) associates with nucleotide-binding oligomerization domain-2 (NOD2) to negatively regulate inflammatory signaling. *J Biol Chem* 286:28574–28583
- Mulhern O, Bowie AG (2010) Unexpected roles for DEAD-box protein 3 in viral RNA sensing pathways. *Eur J Immunol* 40:933–935
- Nace G, Evankovich J, Eid R et al (2012) Dendritic cells and damage-associated molecular patterns: endogenous danger signals linking innate and adaptive immunity. *J Innate Immun* 4:6–15
- Nakamura M, Funami K, Komori A et al (2008) Increased expression of Toll-like receptor 3 in intrahepatic biliary epithelial cells at sites of ductular reaction in diseased livers. *Hepatol Int* 2:222–230
- Nitta S, Sakamoto N, Nakagawa M et al (2012) Hepatitis C virus NS4B protein targets STING and abrogates RIG-I-mediated type-I interferon-dependent innate immunity. *Hepatology*. doi:10.1002/hep.26017
- Oda S, Schroder M, Khan AR (2009) Structural basis for targeting of human RNA helicase DDX3 by poxvirus protein K7. *Structure* 17:1528–1537
- Okamoto K, Moriishi K, Miyamura T et al (2004) Intramembrane proteolysis and endoplasmic reticulum retention of hepatitis C virus core protein. *J Virol* 78:6370–6380
- Oshiumi H, Sasai M, Shida K et al (2003) TIR-containing adapter molecule (TICAM)-2, a bridging adapter recruiting to toll-like

- receptor 4 TICAM-1 that induces interferon-beta. *J Biol Chem* 278:49751–49762
- Oshiumi H, Matsumoto M, Hatakeyama S et al (2009) Riplet/RNF135, a RING finger protein, ubiquitinates RIG-I to promote interferon-beta induction during the early phase of viral infection. *J Biol Chem* 284:807–817
- Oshiumi H, Ikeda M, Matsumoto M et al (2010a) Hepatitis C virus core protein abrogates the DDX3 function that enhances IPS-1-mediated IFN-beta induction. *PLoS One* 5:e14258
- Oshiumi H, Sakai K, Matsumoto M et al (2010b) DEAD/H BOX 3 (DDX3) helicase binds the RIG-I adaptor IPS-1 to up-regulate IFN-beta-inducing potential. *Eur J Immunol* 40:940–948
- Oshiumi H, Miyashita M, Inoue N et al (2010c) The ubiquitin ligase Riplet is essential for RIG-I-dependent innate immune responses to RNA virus infection. *Cell Host Microbe* 8:496–509
- Owsianka AM, Patel AH (1999) Hepatitis C virus core protein interacts with a human DEAD box protein DDX3. *Virology* 257:330–340
- Rathinam VA, Fitzgerald KA (2011) Cytosolic surveillance and antiviral immunity. *Curr Opin Virol* 1:455–462
- Saeed M, Shiina M, Date T et al (2011) In vivo adaptation of hepatitis C virus in chimpanzees for efficient virus production and evasion of apoptosis. *Hepatology* 54:425–433
- Saito T, Owen DM, Jiang F et al (2008) Innate immunity induced by composition-dependent RIG-I recognition of hepatitis C virus RNA. *Nature* 454:523–527
- Sawa Y, Arima Y, Ogura H et al (2009) Hepatic interleukin-7 expression regulates T cell responses. *Immunity* 30:447–457
- Schoggins JW, Wilson SJ, Panis M et al (2011) A diverse range of gene products are effectors of the type I interferon antiviral response. *Nature* 472:481–485
- Schroder M (2009) Human DEAD-box protein 3 has multiple functions in gene regulation and cell cycle control and is a prime target for viral manipulation. *Biochem Pharmacol* 79:297–306
- Schroder M, Baran M, Bowie AG et al (2008) Viral targeting of DEAD box protein 3 reveals its role in TBK1/IKKepsilon-mediated IRF activation. *EMBO J* 27:2147–2157
- Schulz O, Diebold SS, Chen M et al (2005) Toll-like receptor 3 promotes cross-priming to virus-infected cells. *Nature* 433:887–892
- Seth RB, Sun L, Ea CK et al (2005) Identification and characterization of MAVS, a mitochondrial antiviral signaling protein that activates NF-kappaB and IRF 3. *Cell* 122:669–682
- Seya T, Matsumoto M (2009) The extrinsic RNA-sensing pathway for adjuvant immunotherapy of cancer. *Cancer Immunol Immunother* 58:1175–1184
- Seya T, Shime H, Takaki H et al (2012) TLR3/TICAM-1 signaling in RIP3 tumor necroptosis. *Oncoimmunology* 1:917–923
- Shimoda S, Harada K, Niiro H et al (2008) Biliary epithelial cells and primary biliary cirrhosis: the role of liver-infiltrating mononuclear cells. *Hepatology* 47:958–965
- Shimoda S, Harada K, Niiro H et al (2011) Interaction between Toll-like receptors and natural killer cells in the destruction of bile ducts in primary biliary cirrhosis. *Hepatology* 53:1270–1281
- Sillanpaa M, Kaukinen P, Melen K et al (2008) Hepatitis C virus proteins interfere with the activation of chemokine gene promoters and downregulate chemokine gene expression. *J Gen Virol* 89:432–443
- Soulat D, Burckstummer T, Westermayer S et al (2008) The DEAD-box helicase DDX3X is a critical component of the TANK-binding kinase 1-dependent innate immune response. *EMBO J* 27:2135–2146
- Takaoka A, Taniguchi T (2008) Cytosolic DNA recognition for triggering innate immune responses. *Adv Drug Deliv Rev* 60:847–857
- Takaoka A, Yanai H, Kondo S et al (2005) Integral role of IRF-5 in the gene induction programme activated by Toll-like receptors. *Nature* 434:243–249
- Tanabe M, Kurita-Taniguchi M, Takeuchi K et al (2003) Mechanism of up-regulation of human Toll-like receptor 3 secondary to infection of measles virus-attenuated strains. *Biochem Biophys Res Commun* 311:39–48
- Thomas E, Gonzalez VD, Li Q et al (2012) HCV infection induces a unique hepatic innate immune response associated with robust production of type III interferons. *Gastroenterology* 142:978–988
- Uematsu S, Akira S (2007) Toll-like receptors and type I interferons. *J Biol Chem* 282:15319–15323
- Wang N, Liang Y, Devaraj S et al (2009) Toll-like receptor 3 mediates establishment of an antiviral state against hepatitis C virus in hepatoma cells. *J Virol* 83:9824–9934
- Wen C, He X, Ma H et al (2008) Hepatitis C virus infection downregulates the ligands of the activating receptor NKG2D. *Cell Mol Immunol* 5:475–478
- Yeretssian G (2012) Effector functions of NLRs in the intestine: innate sensing, cell death, and disease. *Immunol Res* 54:25–36
- Yoneyama M, Kikuchi M, Natsukawa T et al (2004) The RNA helicase RIG-I has an essential function in double-stranded RNA-induced innate antiviral responses. *Nat Immunol* 5:730–737
- Yoneyama M, Onomoto K, Fujita T (2008) Cytoplasmic recognition of RNA. *Adv Drug Deliv Rev* 60:841–846
- Zeremski M, Petrovic LM, Talal AH (2007) The role of chemokines as inflammatory mediators in chronic hepatitis C virus infection. *J Viral Hepat* 14:675–687
- Zhang Z, Kim T, Bao M et al (2011) DDX1, DDX21, and DHX36 helicases form a complex with the adaptor molecule TRIF to sense dsRNA in dendritic cells. *Immunity* 34:866–878
- Zhu H, Dong H, Eksioglu E et al (2007) Hepatitis C virus triggers apoptosis of a newly developed hepatoma cell line through antiviral defense system. *Gastroenterology* 133:1649–1659

Cleaved/Associated TLR3 Represents the Primary Form of the Signaling Receptor

Florent Toscano,^{*1} Yann Estornes,^{*1} François Virard,^{*} Alejandra Garcia-Cattaneo,[†] Audrey Pierrot,^{*} Béatrice Vanbervliet,^{*} Marc Bonnin,^{*} Michael J. Ciancanelli,[‡] Shen-Ying Zhang,^{‡,§} Kenji Funami,[¶] Tsukasa Seya,[¶] Misako Matsumoto,[¶] Jean-Jacques Pin,^{||} Jean-Laurent Casanova,^{‡,§,#} Toufic Renno,^{*} and Serge Lebecque^{*}

TLR3 belongs to the family of intracellular TLRs that recognize nucleic acids. Endolysosomal localization and cleavage of intracellular TLRs play pivotal roles in signaling and represent fail-safe mechanisms to prevent self-nucleic acid recognition. Indeed, cleavage by cathepsins is required for native TLR3 to signal in response to dsRNA. Using novel Abs generated against TLR3, we show that the conserved loop exposed in LRR12 is the single cleavage site that lies between the two dsRNA binding sites required for TLR3 dimerization and signaling. Accordingly, we found that the cleavage does not dissociate the C- and N-terminal fragments, but it generates a very stable “cleaved/associated” TLR3 present in endolysosomes that recognizes dsRNA and signals. Moreover, comparison of wild-type, noncleavable, and C-terminal-only mutants of TLR3 demonstrates that efficient signaling requires cleavage of the LRR12 loop but not dissociation of the fragments. Thus, the proteolytic cleavage of TLR3 appears to fulfill function(s) other than separating the two fragments to generate a functional receptor. *The Journal of Immunology*, 2013, 190: 764–773.

Toll-like receptors belong to a family of pattern recognition receptors that sense the presence of pathogens and trigger a protective innate immune response (1). These germline-encoded type I integral membrane glycoproteins bind their ligands through their extracellular domain (ECD), which is composed of 19–25 leucine-rich repeats (LRRs) (2). In contrast with other members of the family that primarily recognize molecular patterns specific for nonself invaders, TLR3, TLR7, and TLR9 recognize nucleic acids originating from microbes, as well as from the host. Several fail-safe

mechanisms prevent self-polynucleotide recognition and subsequent autoimmune disorders (3). Ligands must be recognized by cell surface receptor(s) (4) that mediate their internalization before encountering the corresponding TLR exclusively in the acidic endolysosomal compartment from which signal transduction can be initiated (5). Delivery of intracellular TLRs to the endocytic compartments is also tightly regulated by the chaperone Unc93b1 (6, 7). Finally, processing by pH-dependent lysosomal proteases is an additional checkpoint for controlling TLR9 activation (8–10).

Although several studies on intracellular TLRs have been based on TLR9 trafficking and processing, less is known about TLR3. TLR3 appears to be dedicated to the recognition of dsRNA (11), and it plays a central role in the defense against HSV-1 infection in the CNS in humans (12–15). Although endogenous mRNA can activate TLR3 in vitro (16), its involvement in the autoimmune response has not been demonstrated. It was shown that TLR3 dimerization is needed for dsRNA binding and signaling (17). Moreover, analysis of the crystal structure (18, 19) and mutagenesis (18, 20, 21) of TLR3 ECD revealed that dsRNA binding requires interaction of the negatively charged ribose backbone of dsRNA with residues of TLR3 dimers located in LRR1 and LRR3, as well as with a second region formed by LRR19–LRR21 that becomes positively charged in the mildly acidified endolysosomal compartment. Therefore, the requirement for cleavage of the ECD for TLR3 signaling (9, 10, 22) raises an intriguing issue with regard to how endogenous TLR3 is processed and which forms of the receptor recognize dsRNA. In this study, we generated and used novel mAbs directed against TLR3 ECD and mutant forms of TLR3 to demonstrate that cleavage of the LRR12 loop, but not separation of the two fragments, is required for signaling.

^{*}Centre de Recherche en Cancérologie de Lyon, INSERM Unité Mixte de Recherche 1052/Centre National de la Recherche Scientifique 5286, Centre Léon Bérard, 69008 Lyon, France; [†]Institut Curie, INSERM U932, 75005 Paris, France; [‡]St. Giles Laboratory of Human Genetics of Infectious Diseases, Rockefeller Branch, The Rockefeller University, New York, NY 10065; [§]Laboratory of Human Genetics of Infectious Diseases, Necker Branch, INSERM U980, University Paris Descartes, Paris 75015, France; [¶]Department of Microbiology and Immunology, Graduate School of Medicine, Hokkaido University, Kita-ku, Sapporo 060-8638, Japan; ^{||}DENDRITICS SAS, Bioparc Laennec, 69008 Lyon, France; and [#]Pediatric Immunology-Hematology Unit, Necker Hospital for Sick Children, Paris 75015, France

[†]F.T. and Y.E. contributed equally to this work.

Received for publication August 21, 2012. Accepted for publication November 15, 2012.

This work was supported by Cancéropôle Lyon-Auvergne-Rhône-Alpes.

F.T., Y.E., F.V., A.G.-C., M.J.C., S.-Y.Z., T.S., M.M., T.R., and S.L. designed the experiments. F.T., Y.E., F.V., A.G.-C., A.P., B.V., S.-Y.Z., M.J.C., M.B., K.F., and J.-J.P. performed experiments and analyzed data. F.T., Y.E., F.V., J.-L.C., T.R., and S.L. wrote the manuscript, with all authors providing detailed comments and suggestions. S.L. directed the project.

Address correspondence and reprint requests to Prof. Serge Lebecque, Centre de Recherche en Cancérologie de Lyon, INSERM Unité Mixte de Recherche 1052/Centre National de la Recherche Scientifique 5286, Centre Léon Bérard, 28 rue Laennec, 69008 Lyon, France. E-mail address: serge.lebecque@univ-lyon1.fr

The online version of this article contains supplemental material.

Abbreviations used in this article: DC, dendritic cell; ECD, extracellular domain; EEA, early endosome Ag; EndoH, endoglycosidase H; ER, endoplasmic reticulum; FL, full length; HA, hemagglutinin; HMW, high molecular weight; LMW, low molecular weight; LRR, leucine-rich repeat; mDC, monocyte-derived dendritic cell; NSCLC, non-small cell lung cancer; PNGase, peptide-N-glycosidase F; Poly(A:U), polyadenylic-polyuridylic acid; Poly(I:C), polyinosinic-polycytidylic acid; siRNA, small interfering RNA; WT, wild-type.

Copyright © 2013 by The American Association of Immunologists, Inc. 0022-1767/13/\$16.00

www.jimmunol.org/cgi/doi/10.4049/jimmunol.1202173

type I (Invitrogen) and fibronectin (Sigma)-coated dishes. CD14⁺ monocytes were purified from peripheral blood of healthy donors: PBMCs were isolated from human peripheral blood by standard density-gradient centrifugation on Pancoll (PAN Biotech) and then mononuclear cells were separated from PBLs on a 50% Percoll solution (GE Healthcare). Monocytes were enriched by one step of adherence and differentiated in immature dendritic cells (DCs) in complete RPMI 1640 medium supplemented with 200 ng/ml human GM-CSF (kind gift of Schering-Plough) and 50 ng/ml human rIL-4 (R&D Systems) for 6 d. NCI-H292 and NCI-H1703 non-small cell lung cancer (NSCLC) cell lines (American Type Culture Collection) were grown in RPMI 1640 medium (Invitrogen) supplemented with 10% FBS (Sigma), HEPES, NaPy, 100 U/ml penicillin/streptomycin, and 2 mM glutamine. THP1 and U937 cell lines were grown in RPMI 1640 medium (Invitrogen) supplemented with 10% FBS and 100 U/ml penicillin/streptomycin. IFN- α was from Schering-Plough. Z-FA-fmk, chloroquine, tunicamycin, and cycloheximide were from Sigma. Polyinosinic-polycytidylic acid [Poly(I:C)]-high molecular weight (HMW) and Poly(I:C)-low molecular weight (LMW) were purchased from InvivoGen. polyadenylic-polyuridylic acid [Poly(A:U)] was from Innate Pharma. Mouse monoclonal IgG1 anti-actin Ab was from MP Biomedicals. Anti-mouse TLR3 Ab T3.7C3 was a gift from Nadège Goutagny (Centre de Recherche sur le Cancer de Lyon, Lyon, France). HRP-conjugated donkey anti-mouse secondary Ab was from Jackson ImmunoResearch.

TLR3.2 and TLR3.3 Ab preparation and purification

BALB/C mice were immunized with recombinant human TLR3 ECD (R&D Systems) by three i.p. injections of the immunogen in the presence of Freund's adjuvant and a final i.v. boost, 3 d before spleen isolation. Splenic cells were fused with the SP20 myeloma cell line in the presence of polyethylene glycol. Hybridoma supernatants were screened by immunofluorescent staining of pUNO-hTLR3-HA and pUNO-hTLR3-V5 transiently transfected 293T cells with Exgen 500 (Euromedex) and fixed with acetone. Only clones recognizing both transfected cells were selected.

Western blotting

Cells were lysed in cold lysis buffer (20 mM Tris-HCl [pH 7.4], 150 mM NaCl, 0.2% Nonidet P-40, supplemented with 1 mM orthovanadate, 10 mM NaF, and a protease inhibitor mixture; Sigma) for 25 min on ice. Cell lysates were cleared by centrifugation (13,000 \times g for 10 min at 4°C), and protein concentration was determined using the Bradford assay (Bio-Rad). Protein lysates were denatured or not in Laemmli buffer containing 1% SDS and 5 mM DTT and heated to 95°C for 5 min. For peptide-N-glycosidase F (PNGase)/endoglycosidase H (EndoH) digestions, lysates were treated as recommended by the manufacturer (New England BioLabs). Proteins were resolved on SDS-polyacrylamide gels and transferred onto polyvinylidene difluoride membranes by electroblotting, and nonspecific binding sites were blocked using TBS containing 0.1% Tween-20 and 5% (w/v) dry milk. After incubation with the appropriate secondary Abs conjugated to HRP, blots were revealed using ECL (GE Healthcare) or SuperSignal (Thermo Scientific) reagents. For reimmunoprecipitation experiments, anti-TLR3 or anti-HA immunoprecipitates were eluted with preheated lysis buffer containing 1% SDS and 5 mM DTT; 20% of each sample was resolved by SDS-PAGE, and the remaining 80% was diluted 10-fold in lysis buffer and then reimmunoprecipitated with TLR3.2 or anti-HA Ab, resolved by SDS-PAGE, and analyzed with either TLR3.2 or TLR3.3 Ab.

Immunofluorescence

Cells were washed with PBS, fixed with 4% formaldehyde for 10 min at room temperature, and washed three times with PBS. Cells were then blocked using Image-iT FX signal enhancer (Life Technologies) for 30 min at room temperature and washed once with PBS. Thereafter, each washing step was done using TBS. Cells were incubated for 1 h at room temperature with TLR3.1, anti-HA, anti-calreticulin, early endosome Ag (EEA)1, or Lamp1 (Abcam) primary Abs. After washing three times, cells were incubated for 30 min at room temperature with secondary Abs (goat anti-mouse-Alexa Fluor 488 and goat anti-rabbit-Alexa Fluor 555 or Alexa Fluor 633; Life Technologies). Cells were washed again 3 min each. Cover slips were air-dried and then mounted using ProLong Gold antifade reagent with DAPI (Life Technologies). Images were acquired using a confocal microscope (Zeiss Axiovert 100 M LSM510) with a 1.4 NA Plan-Apochromat 63 \times oil-immersion lens. Image noise was reduced using a Despeckle Fiji filter.

Cytokines measurement

The supernatant from NCI-H292 and NCI-H1703 cells, cultured or not with 100 μ g/ml Poly(I:C) for 24 h, was assayed for IL-6, IP-10, and RANTES

using a MILLIPLEX MAP kit (Millipore) on a Luminex Bio-Plex 200 System Analyzer (Bio-Rad). The supernatant from monocyte-derived DCs (mDCs), cultured or not with 100 μ g/ml Poly(I:C) for 24 h, was assayed for IL-6, IP-10, TNF- α , and IFN- λ using a Quantikine ELISA test (R&D Systems), as described by the manufacturer.

DNA cloning

Preparation of the LRR1-11 and 13-21 deletion mutants was described previously (23). For the TLR3-Ins12-HA mutant, mutagenesis was performed using the QuikChange XL Site-Directed Mutagenesis Kit (Stratagene) and primer pairs containing deletion of 24 nucleotides: 5'-CTGAATTTGAAACG-GTCTTTACTCTCCCAAGATTGATGATTTTCT-3' (forward) and 5'-AGAAAAATCATCAATCTTGGGGAGAGTAAAAGACC GTTTCAAA-TTCAG-3' (reverse). Ten nanograms of plasmid DNA and 125 ng of primers were used, according to the manufacturer's instructions. Two colonies from each library were sequenced.

For the TLR3-Cter₃₅₆-HA mutant, LRR deletion mutants of TLR3 (A₂₂-K₃₅₆) were generated by PCR with Phusion (Finnzyme), using the appropriate primers: 5'-TGTTTGGAGCACCTTAACATGGAAG-3' (forward) and 5'-GGTGGAGGATGCACACAGCATCCCA-3' (reverse). PCR was performed with the following cycling conditions: 10 s at 98°C, 2 min at 72°C for 25 cycles. The PCR product was treated with DpnI to digest the template DNA, phosphorylated with T4 PNK (New England BioLabs), and ligated using a DNA Ligation kit (New England BioLabs). Deletion constructs were sequenced. TLR3-Cter₃₄₆ was provided by P. Bénaroch (Curie Institute, Paris, France).

RNA interference

Synthetic TRIF (L-012833-00-0005) and control nonsilencing (D-001810-03-20) small interfering RNAs (siRNAs) were from Dharmacon. TLR3 Stealth RNAi siRNA (TLR3HSS110816) was from Invitrogen. siRNAs mix was prepared in Opti-MEM medium (Invitrogen), and cells in suspension were transfected using HiPerFect reagent (QIAGEN), as described by the manufacturer. The final siRNA concentrations were 25 nM. Transfected cells were seeded in 6-well plates or 96-well white plates (Greiner) and incubated for 24 h. Medium was replaced with fresh complete medium, and cells were incubated for 48 h before Poly(I:C) treatment.

Generation of ISRE- and NF- κ B-luciferase reporter cell lines

HEK293, NCI-H292, and NCI-H1703 cells were transfected with luciferase ISRE- or NF- κ B-reporter lentiviruses (SABiosciences), according to the manufacturer's recommendations, and transduced cells were selected with puromycin.

Reporter luciferase assays

Cells were seeded in white 96-well plates (10,000 cells/well); 24 h later they were treated with 10 μ g/ml poly(I:C) in 50 μ l medium for 4 or 6 h, depending on the cell line. Then, 50 μ l Steady-Glo reactive (Promega) was added to each well before reading luminescence with a Tecan Infinite 200 microplate reader using i-control software (Tecan).

Transient expression in HEK293 cells

Cells were seeded in 100-mm dishes to reach ~70% confluence on the day of transfection. Cells were transfected with pUNO, TLR3-wild-type (WT)-HA, TLR3-Ins12-HA, TLR3-Cter₃₅₆-HA, or TLR3-Cter₃₄₆-HA by incubating 8 μ l Lipofectamine 2000 (Invitrogen) with 8 μ g plasmid in 6 ml Opti-MEM medium for 5 h; subsequently, Opti-MEM was replaced by fresh medium. Twenty-four hours after transfection, cells were trypsinized and seeded in 96-well white plates and 6-well plates and incubated for 24 h.

Stable transfections

P2.1 cells were transfected with pUNO-hTLR3 vectors, which contain WT TLR3 cDNA, TLR3-Ins12 mutant, or TLR3-Cter₃₅₆ mutant cDNA, or with an empty mock vector, in the presence of Lipofectamine Reagent (Invitrogen) and PLUS Reagent (Invitrogen), as described by the manufacturer. Stable transfectants were selected with medium containing blasticidin (5 μ g/ml; Invitrogen). The presence of TLR3 was confirmed by Western blotting.

Determination of mRNA levels by RT-quantitative PCR

Total RNA was extracted from P2.1 cells. RNA was reverse-transcribed using Oligo-deoxy-thymidine. To determine mRNA levels for IL-29, quantitative PCR was performed with Assays-on-Demand probe/primer combinations and 2 \times universal reaction mixture in an ABI Prism 7700 Sequence Detection System (all from Applied Biosystems). The β -glucuronidase (GUS) gene was used for normalization. Results are expressed according to the Δ Ct method, as described by the manufacturer.

Coimmunoprecipitation

Cells were cultured in 150-mm dishes, collected, washed in PBS, and lysed in 750 μ l cold lysis buffer (20 mM Tris-HCl [pH 7.4], 150 mM NaCl, 0.2% Nonidet P-40, supplemented with 1 mM orthovanadate, 10 mM NaF, and a protease inhibitor mixture; Sigma) for 25 min on ice. Cell lysates were cleared by centrifugation (13,000 \times g for 10 min at 4°C). Lysates were precleared with 50 μ l Sepharose-6B (Sigma) for 1 h at 4°C and then immunoprecipitated overnight at 4°C with 5 μ g mouse anti-TLR3.2, anti-TLR3.3, or control IgG1 Ab (R&D Systems) and the following day in the presence of 20 μ l protein G-Sepharose for 3 h at 4°C. Beads were recovered by centrifugation, and immunoprecipitates were washed extensively with lysis buffer and eluted with Laemmli buffer containing 1% SDS and 5 mM DTT and heated to 95°C for 10 min.

TLR3 ECD modeling

The MacPyMOL software (DeLano Scientific) was used to generate the 3D representation of the TLR3 structure shown on Figs. 1C and 5A (PDB:1ZIW).

Statistical analysis

Statistical significance was determined using the Student *t* test.

Results

Profiling endogenous TLR3 expression

To analyze the biology of endogenous TLR3, we generated three new mAbs (designated as TLR3.1, TLR3.2, and TLR3.3) raised against the ECD of the receptor. First, the Abs were validated using HEK293 cells stably expressing TLR3 tagged with a C-terminal HA epitope (HEK293-TLR3-HA). In this model, Western blots probed with anti-HA, TLR3.2, and TLR3.3 Abs revealed an ~130 kDa band corresponding to the expected molecular mass of highly glycosylated TLR3 (Fig. 1A) (24). The stronger signal observed with TLR3.2 suggested that this Ab has a higher affinity for TLR3 than does TLR3.3. In addition, anti-HA and TLR3.2 Abs stained

a second band at ~72 kDa similar to the C-terminal fragment of TLR3 observed after cleavage by cathepsin. In addition, TLR3.3 Ab detected a third band (Fig. 1A) not recognized by anti-HA mAb and with a size ~60 kDa that could represent the N-terminal fragment of cleaved TLR3. TLR3.1 Ab did not detect TLR3 by Western blot, but it showed the same staining by immunofluorescence as observed with anti-HA Ab (Fig. 1B, Supplemental Fig. 1A). To unequivocally identify the different bands revealed by TLR3.2 and TLR3.3 Abs on Western blot, we mapped the recognized epitopes using 20 single LRR-deleted forms of the ECD of TLR3 (LRR1–11 and LRR13–21) (23). Fig. 1C establishes that TLR3.2 Ab recognizes an epitope present in LRR20, whereas TLR3.3 binds to an epitope formed by residues present in LRR7 and LRR8. We next verified whether similar expression profiles could be observed in human cells of different origins and wondered how treatment with IFN- α , which is known to upregulate the expression of TLR3 (25), would modify this pattern. We determined TLR3 expression by immunoblot of lysates from mDCs (Fig. 1D), from human monocytic cell lines U937 and THP1 (Supplemental Fig. 1B, 1C), and from human bronchial epithelial cells transformed by SV40-T Ag (BEAS-2B; Supplemental Fig. 1D) or derived from NSCLC (NCI-H292 and NCI-H1703; Fig. 1E). The three forms of TLR3 (130, 72, and 60 kDa) were present in every lysate with the exception of THP1, which did not appear to express TLR3 (Supplemental Fig. 1B) or respond to Poly(I:C) (Supplemental Fig. 1E). Resting MRC-5 cells were also devoid of TLR3, but kinetic analysis showed that IFN- α treatment led first to the detection of the high molecular mass bands (~130 and ~135 kDa) of TLR3, followed by an increase in the intensity of the lower ~72-kDa molecular mass band detected by TLR3.2 mAb (Fig. 1F), suggesting that the former might

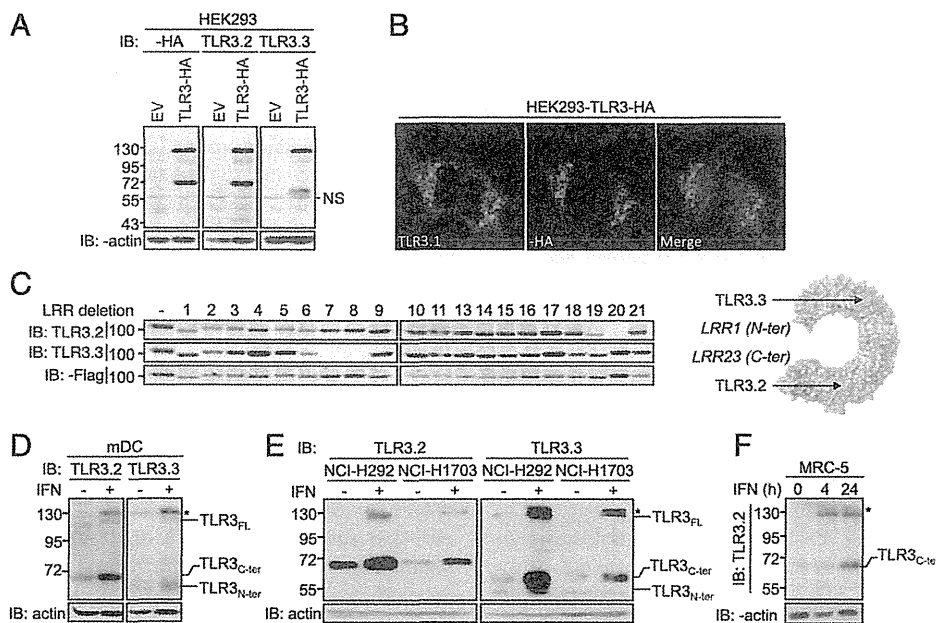


FIGURE 1. Profiling endogenous TLR3 expression. (A) Immunoblot analysis of HEK293 cells stably expressing an empty vector (EV) or TLR3-HA; lysates were analyzed with monoclonal anti-HA, TLR3.2, TLR3.3, and anti-actin Abs. (B) Immunofluorescence of HEK293 cells stably expressing TLR3-HA; cells were stained with anti-HA or TLR3.1 Abs, followed by DAPI nuclear staining (blue). Original magnification \times 63. (C) *Left panel*, Epitope mapping of TLR3.2 and TLR3.3 Abs on HEK293 cells stably transfected with TLR3-HA WT (–) or TLR3-HA mutants carrying LRR deletions (1–11 and 13–21, as indicated). Lysates were analyzed with monoclonal TLR3.2, TLR3.3, and anti-Flag Abs, as indicated. *Right panel*, Schematic representation of epitopes recognized by TLR3.2 and TLR3.3 Abs on TLR3 ECD. (D) Immunoblot analysis of mDCs treated (+) or not (–) for 18 h with IFN- α (1000 IU/ml); lysates were analyzed with TLR3.2, TLR3.3, and anti-actin Abs. (E) Immunoblot analysis of NCI-H292 and NCI-H1703 cells treated (+) or not (–) for 18 h with IFN- α (1000 IU/ml); lysates were analyzed with TLR3.2, TLR3.3, and anti-actin Abs. (F) Immunoblot analysis of MRC-5 cells treated (+) or not (–) for the indicated times with IFN- α (1000 IU/ml); lysates were analyzed with TLR3.2 and anti-actin Abs. Values in (A) and (C)–(F) represent molecular mass (kDa). All data are representative of at least three independent experiments. NS, Nonspecific band.

represent the precursors of the latter. In other cell lines, the absolute and relative intensities of the three bands varied depending on the origin of the cells, the Ab used, and the treatment with IFN- α . However, under basal conditions, all cells primarily expressed the 72 and 60 kDa TLR3 forms. Treatment with IFN- α increased the intensity of the three bands and allowed the detection of a higher molecular mass form \sim 135 kDa in mDCs and in the four cell lines analyzed (asterisk in Fig. 1D–F and Supplemental Fig. 1D). In conclusion, our data suggest that human TLR3 is spontaneously cleaved into a C-terminal fragment \sim 72 kDa recognized by TLR3.2 and a C-terminal fragment \sim 60 kDa recognized by TLR3.3, and the relative abundance of cleaved versus uncleaved TLR3 appears to vary with the cell under consideration.

TLR3 ECD cleavage by cathepsins generates two remarkably stable fragments

To further explore the processing of endogenous TLR3 and its functional consequences, we selected the NCI-H292 and NCI-H1703 NSCLC cell lines, which triggered an innate immune response when stimulated with Poly(I:C), as indicated by cytokine secretion (Supplemental Fig. 2A) and by activation of ISRE-dependent luciferase reporter genes (Supplemental Fig. 2B). We ascertained that this response was mediated exclusively by TLR3 by showing its strict dependence on TRIF, the only known adaptor for TLR3 (Supplemental Fig. 2B). We started analyzing the effects of the cathepsin inhibitor Z-FA-fmk on the expression of the different forms of TLR3. Following Z-FA-fmk treatment, the 130 kDa band became more intense with time, whereas the 72 and 60 kDa bands gradually disappeared in both NCI-H292 and NCI-H1703 cells (Fig. 2A, Supplemental Fig. 2C, respectively), as well as in HEK293-TLR3-HA cells (Fig. 2B). These results confirm that cathepsins are necessary for TLR3 cleavage in epithelial cells (22). In NCI-H292 cells, the accumulation of full-length TLR3 was observed as early as 120 min after the addition of Z-FA-fmk (Fig. 2C), whereas in the three cell lines both C-terminal (TLR3_{C-ter}) and N-terminal (TLR3_{N-ter}) TLR3 fragments disappeared with an apparent $t_{1/2} > 24$ h (Fig. 2A, 2B, Supplemental Fig. 2C). Of note, Z-FA-fmk induces a shift of TLR3 full-length (TLR3_{FL}) from 130 kDa to 135 kDa (TLR3_{FL+}) in both NSCLC cell lines, which is more visible after prolonged gel migration (Fig. 2D). This TLR3_{FL+} could represent the fully glycosylated form of TLR3 leaving the post-Golgi cisternae and not cleaved yet. Published data with regard to the effects of cathepsin inhibitors on TLR3 signaling seem contradictory (8, 9). In this study, we observed that ISRE- and NF- κ B-dependent responses to Poly(I:C) were not modified after prolonged treatment with Z-FA-fmk in NCI-H292 cells (Supplemental Fig. 2D), whereas they were significantly, but not completely, suppressed in NCI-H1703 cells (Supplemental Fig. 2E). However, considering the much higher level of TLR3 expression in resting NCI-H292 cells than in NCI-H1703 cells (Fig. 1E), the amounts of TLR3_{C-ter} detected in NCI-H292 cells after 72 h of treatment with Z-FA-fmk was still comparable to the basal level in NCI-H1703 cells. Therefore, these results suggest that cleaved TLR3 is important for signaling, although uncleaved TLR3 might still transduce some signal. Importantly, Z-FA-fmk treatment blocked TLR3 cleavage and Poly(I:C)-induced cytokine secretion in mDCs (Fig. 2E, 2F) and TR3 signaling in macrophages U937 cells (Fig. 2G, Supplemental Fig. 2F), whereas the response to TNF- α was unaffected. Like with Z-FA-fmk treatment, exposure to the lysosomotropic weak base chloroquine, which prevents cathepsin activity, led to the accumulation of TLR3_{FL+} within 3 h and to the reciprocal disappearance of the two TLR3 fragments in NCI-H292 (Fig. 2H) and NCI-H1703 (Supplemental Fig. 2G) cells after 48 h. The same results

were obtained with the specific inhibitor of vacuolar H⁺ ATPase Bafilomycin (data not shown). Furthermore, short-term blockade of de novo protein synthesis with cycloheximide confirmed the relative high stability of endogenous TLR3_{C-ter} (apparent $t_{1/2} > 24$ h) (Fig. 2I, 2J) compared with TLR3_{FL} (apparent $t_{1/2} < 4$ h). Despite a weaker signal, a half-life similar to TLR3_{C-ter} was estimated for TLR3_{N-ter} (Fig. 2H, Supplemental Fig. 2G). Altogether, our data indicate that, in resting cells, TLR3 is actively transcribed and rapidly cleaved by cathepsins upon its transfer in endolysosomes into two highly stable proteolytic fragments, in agreement with a very recent report (26).

TLR3 transits steadily through the Golgi before being cleaved in the endolysosomal compartments

Although TLR3, like other intracellular TLRs, depends on the chaperone protein Unc93b1 for proper trafficking, it is unclear whether its transfer to the endolysosomes occurs constitutively or in response to its ligand. Using TLR3.1 Ab, we observed by immunofluorescence microscopy that TLR3 colocalizes extensively with Lamp1 (a lysosome marker) but not with EEA1 (an early endosome marker) (Fig. 3A, Supplemental Fig. 3) in resting epithelial cells and that the level of colocalization remained unchanged after stimulation with dsRNA (Supplemental Fig. 3). We next addressed the trafficking of TLR3 by analyzing the N-glycosylation status of the protein, which represents \sim 35% of its total mass (24). After treatments of cell lysates with PNGase, which removes all N-glycans, TLR3_{FL} and TLR3_{FL+} shifted from 130 and 135 kDa, respectively, to 95 kDa (Fig. 3B, 3C), corresponding to the expected molecular mass of nonglycosylated neosynthesized TLR3_{FL} (904 aa). The TLR3_{C-ter} band shifted from 72 to 50 kDa, indicating that both cleaved and noncleaved TLR3 are glycosylated. Treatment with EndoH, an endoglycosidase that cleaves N-glycans before their further modification in the Golgi apparatus, indicates that noncleaved TLR3_{FL} is EndoH sensitive, whereas TLR3_{FL+} and TLR3_{C-ter} are partially EndoH resistant. This was similar to the presence of hybrid glycans on TLR9 even after trafficking through the Golgi (27). Cell treatment with tunicamycin, a de novo N-glycosylation inhibitor, caused the rapid fading of TLR3_{FL} (apparent $t_{1/2} < 8$ h) and the appearance of a band at \sim 95 kDa representing neosynthesized nonglycosylated full-length TLR3 (Fig. 3D, 3E). Altogether, our data indicate that TLR3_{FL} corresponds to the small amounts of TLR3 present in the endoplasmic reticulum (ER), which is steadily translocated to the Golgi in resting cells, converted into fully glycosylated TLR3_{FL+}, and exported to the endosomes/lysosomes, where it is rapidly cleaved.

The endolysosomal pool of cleaved TLR3 is sufficient for signaling

To determine which forms of endogenous TLR3 are functional, we started using specific siRNA and took advantage of the prolonged stability of cleaved fragments versus TLR3_{FL}. We observed that 24 and 48 h after transfection, TLR3_{FL} had completely disappeared, whereas the two cleavage fragments were still abundant (Fig. 4A, Supplemental Fig. 4A). Under these conditions, the Poly(I:C)-induced ISRE-dependent response was not reduced (Fig. 4B), suggesting that the uncleaved TLR3_{FL} does not contribute significantly to downstream signaling, probably because of its weak expression compared with the cleaved fragments from the beginning of the experiment. Indeed, ISRE activation faded away gradually with time as the presence of cleaved TLR3 decreased (Fig. 4A, 4B). Similar results were obtained with a NF- κ B-dependent reporter gene (Supplemental Fig. 4B). These data show that cleaved TLR3 can signal in the absence of uncleaved TLR3_{FL} and may even represent the predominant signaling form of the receptor.

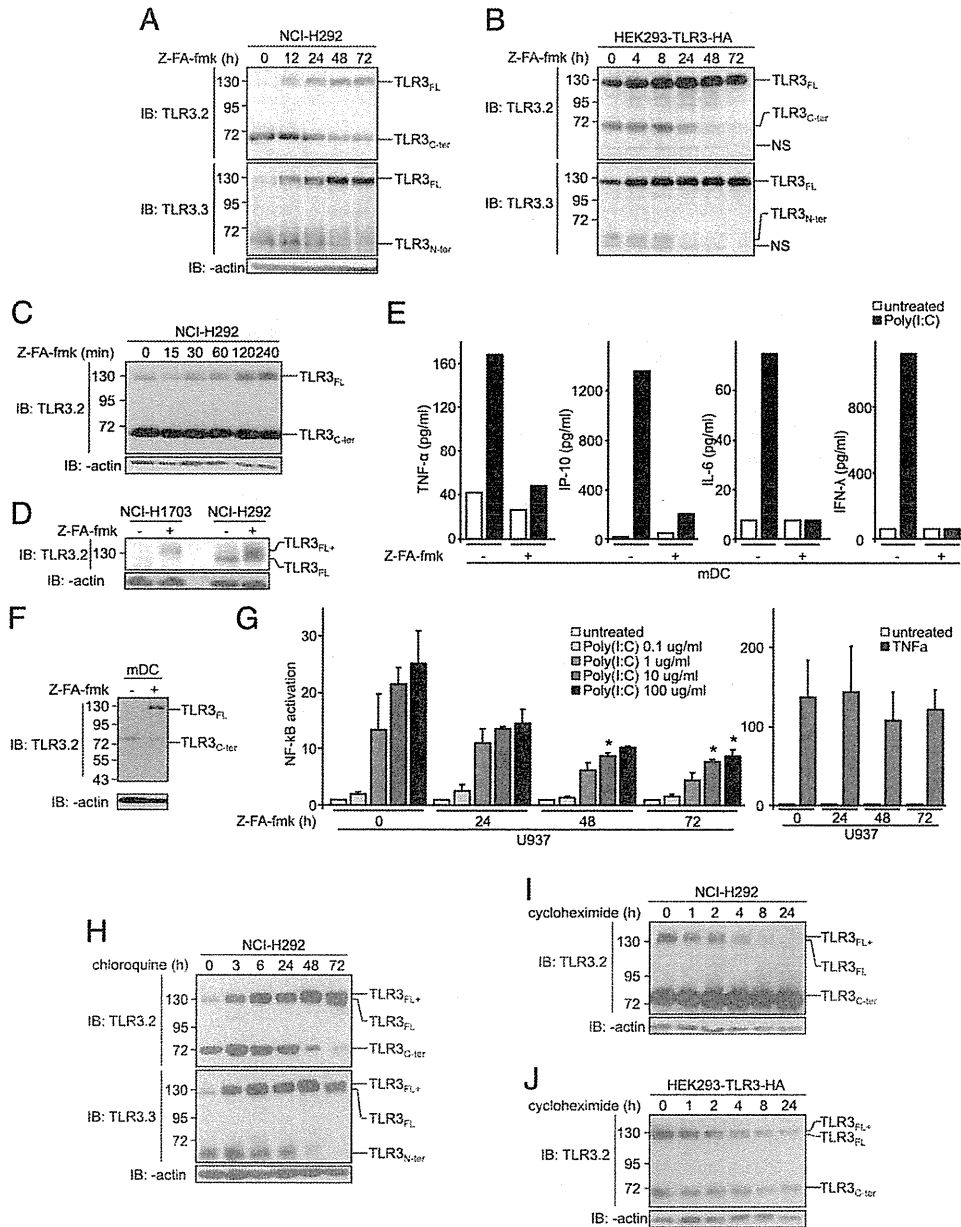


FIGURE 2. Cleavage by cathepsins generates two TLR3 stable fragments. **(A)** Immunoblot analysis of NCI-H292 cells treated for the indicated times with Z-FA-fmk (20 μM) renewed every 24 h. Lysates were analyzed with TLR3.2, TLR3.3, and anti-actin Abs. **(B)** Immunoblot analysis of HEK293-TLR3-HA cells treated for the indicated times with Z-FA-fmk (20 μM) renewed every 24 h. Lysates were analyzed with TLR3.2 and TLR3.3 Abs. **(C)** Immunoblot analysis of NCI-H292 cells treated for the indicated times with Z-FA-fmk (20 μM). Lysates were analyzed with TLR3.2 and anti-actin Abs. **(D)** Immunoblot analysis of NCI-H292 and NCI-H1703 cells treated for 24 h with Z-FA-fmk (20 μM). Lysates were analyzed with TLR3.2 and anti-actin Abs. **(E)** Cytokine production in mDCs that were pretreated for 48 h with Z-FA-fmk and then treated with Poly(I:C) (10 μg/ml) for 24 h. **(F)** Immunoblot analysis of mDCs that were pretreated for 72 h with Z-FA-fmk (20 μM); lysates were analyzed with TLR3.2 and anti-actin Abs. **(G)** NF-κB reporter assay in U937 cells that were pretreated for the indicated times with Z-FA-fmk (20 μM), renewed every 24 h, and then treated with Poly(I:C) at the indicated concentrations (*left panel*) or with TNF-α (50 ng/ml) (*right panel*) for 4 h. **(H)** Immunoblot analysis of NCI-H292 cells treated for the indicated times with chloroquine (1 μg/ml). Lysates were analyzed with TLR3.2, TLR3.3, and anti-actin Abs. **(I)** Immunoblot analysis of NCI-H292 cells treated for the indicated times with cycloheximide (1.5 μg/ml). Lysates were analyzed with TLR3.2 and anti-actin Abs. **(J)** Immunoblot analysis of HEK293-TLR3-HA cells treated for the indicated times with cycloheximide (1.5 μg/ml). Lysates were analyzed with TLR3.2 and anti-actin Abs. Values represent molecular mass (kDa). Data are mean (G) or representative (A–F, H–J) of at least three independent experiments. **p* < 0.05, untreated cells versus Z-FA-fmk-treated cells.

The N- and C-terminal fragments of TLR3 ECD are needed for efficient signaling

To definitely establish the functionality of uncleaved versus cleaved TLR3, we expressed three mutants of TLR3 in HEK293 cells. Given the apparent molecular mass of deglycosylated TLR3_{C-ter} and TLR3_{FL} (50 and 95 kDa, respectively; Fig. 3B, 3C), the highly

conserved insertion within LRR12, which protrudes on the glycosylation-free side of LRR12 (residues 335–342) (28–31), was a likely site for proteolysis. Thus, the first mutant lacked the entire LRR12 insertion (TLR3-Ins12-HA), whereas the two others represented the C-terminal fragment starting just at the end of the LRR12 insertion (aa 346: TLR3-Cter₃₄₆-HA), as established and

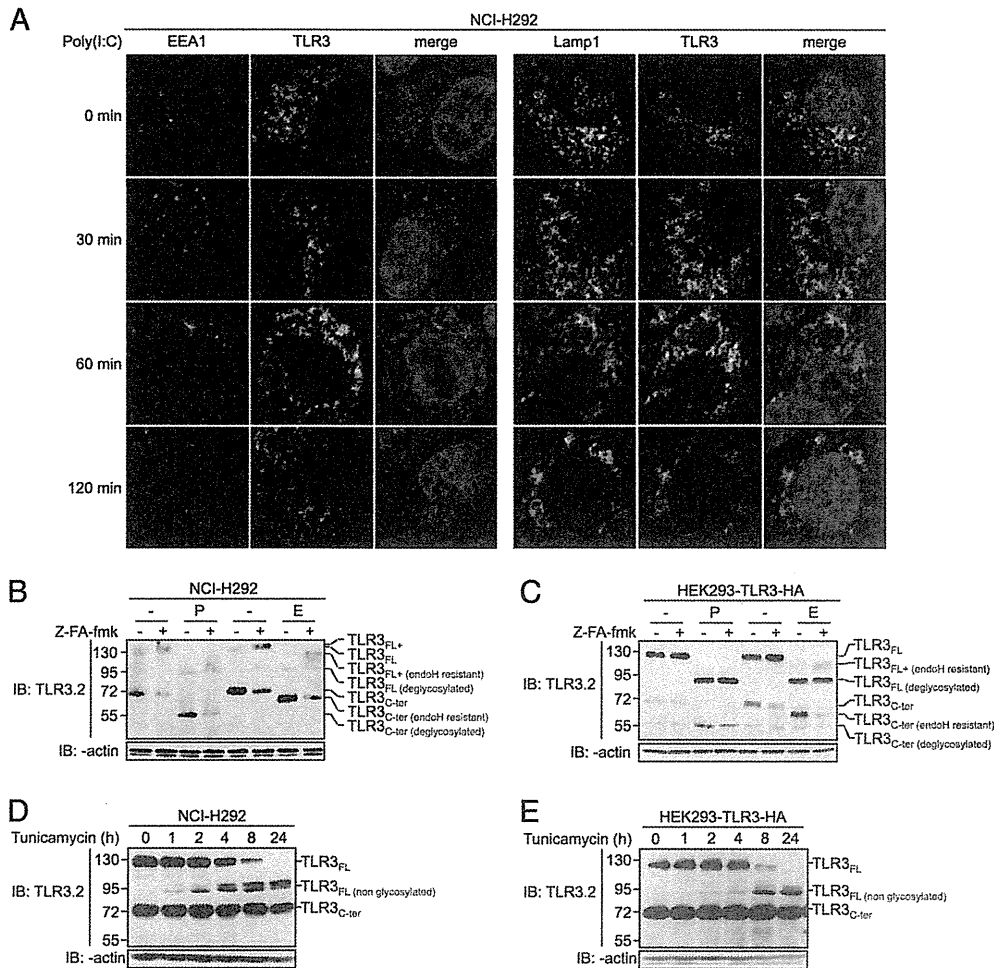


FIGURE 3. TLR3 transits through the Golgi before being cleaved in the endolysosomal compartments. **(A)** Immunofluorescence of NCI-H292 cells treated for the indicated times with Poly(I:C) (10 μ g/ml) and then stained with EEA1 or Lamp1, and TLR3.1 Abs, followed by DAPI nuclear staining (blue). Original magnification $\times 63$. **(B)** Immunoblot analysis of NCI-H292 cells that were treated or not with Z-FA-fmk (20 μ M) for 24 h. Lysates were left untreated (–) or were treated (+) with PNGase (P) or EndoH (E) and then analyzed with TLR3.2 and anti-actin Abs. **(C)** Immunoblot analysis of HEK293-TLR3-HA cells that were treated or not with Z-FA-fmk (20 μ M) for 24 h. Lysates were left untreated (–) or were treated (+) with PNGase (P) or EndoH (E) and then analyzed with TLR3.2 and anti-actin Abs. **(D)** Immunoblot analysis of NCI-H292 cells that were treated for the indicated times with tunicamycin (1 μ g/ml). Lysates were analyzed with TLR3.2 and anti-actin Abs. **(E)** Immunoblot analysis of HEK293-TLR3-HA cells that were treated for the indicated times with tunicamycin (1 μ g/ml). Lysates were analyzed with TLR3.2 and anti-actin Abs. Values in (B)–(D) represent molecular mass (kDa). Data are representative of at least three independent experiments.

characterized by Garcia-Cattaneo et. al (22), or at the beginning of LRR13 (aa 356: TLR3-Cter₃₅₆-HA) (Fig. 5A). Immunoblots confirmed that all three constructs were expressed at comparable levels in HEK-293T-transfected cells (Fig. 5B), with TLR3-Ins12-HA expressed as a single 130-kDa band, confirming that the LRR12 insertion contains the cleavage site and that TLR3-Ins12-HA is a noncleavable form of the receptor. As expected, lysates from TLR3-Cter₃₅₆-HA- or TLR3-Cter₃₄₆-HA-transfected

cells contained a single form ~ 72 kDa, whose size is consistent with the predicted length of each construct (Fig. 5B). We also observed that treatment with Poly(I:C) did not modify the processing of TLR3 and, particularly, did not induce the cleavage of TLR3-Ins12-HA (Fig. 5B).

When expressed in HEK293 cells, the noncleavable form of the receptor showed the capacity to activate ISRE- and NF- κ B-dependent transcription in response to 10 μ g/ml of Poly(I:C) (Fig. 5C)

FIGURE 4. Endogenous cleaved TLR3 is sufficient to fully signal. **(A)** Immunoblot analysis of NCI-H292 cells at the indicated times after non-silencing (–) or TLR3 (+) siRNA transfections (25 μ M). Lysates were analyzed with TLR3.2 and anti-actin Abs. **(B)** ISRE reporter assay in NCI-H292 cells at the indicated times after non-silencing (–) or TLR3 (+) siRNA transfections (25 μ M) and treatment without or with Poly(I:C) (10 μ g/ml) for 4 h. Data are representative (A) or the mean (B) of three independent experiments. Error bars represent SEM. * $p < 0.05$, untreated cells versus Poly(I:C)-treated cells.

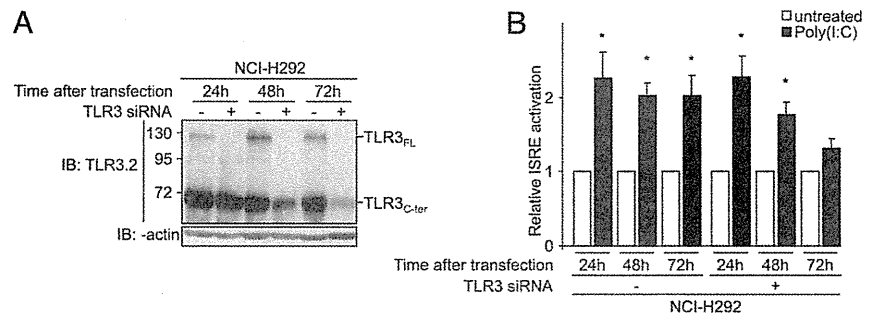
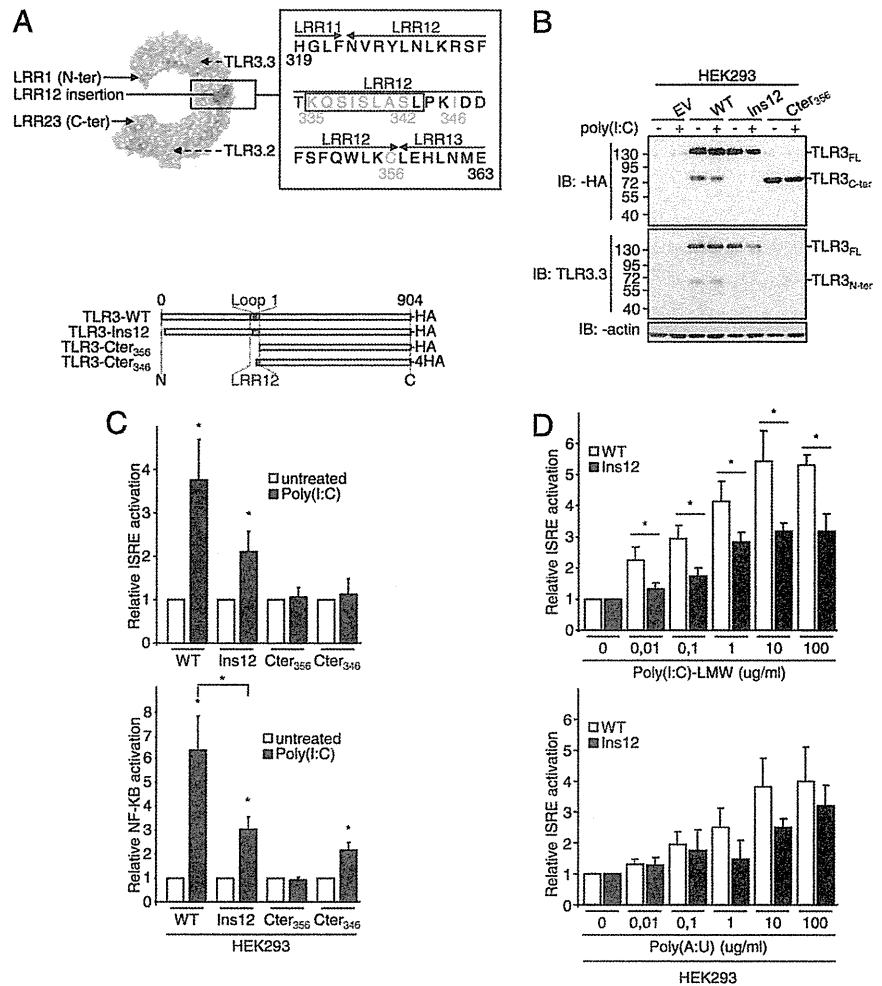


FIGURE 5. Noncleaved TLR3 can signal but the isolated C-terminal TLR3 fragment cannot. **(A)** Upper panel, Model of the putative location of the cleavage on LRR12 and TLR3 sequence with starting points of TLR3-Cter₃₅₆ and TLR3-Cter₃₄₆ mutants and deleted sequence (aa 335–342) of TLR3-Ins12 (in red). Blue framework: LRR12 loop1. Lower panel, Schematic representation of TLR3 mutants. **(B)** Immunoblot analysis of HEK293 cells transfected with empty vector (EV), TLR3-WT-HA (WT), TLR3-Ins12-HA (Ins12), or TLR3-Cter₃₅₆-HA (Cter₃₅₆) and then treated without (–) or with (+) Poly(I:C) (10 μg/ml) for 4 h. Lysates were analyzed with anti-HA, TLR3.3, and anti-actin Abs. Values represent molecular mass (kDa). **(C)** ISRE (upper panel) and NF-κB (lower panel) reporter assay in HEK293 cells transfected with TLR3-WT-HA, TLR3-Ins12-HA, TLR3-Cter₃₅₆-HA (Cter₃₅₆), or TLR3-Cter₃₄₆-HA (Cter₃₄₆), and then treated without (white) or with (black) Poly(I:C) (10 μg/ml) for 6 h. **(E)** ISRE reporter assay in HEK293 cells transfected with TLR3-WT-HA or TLR3-Ins12-HA and then treated with the indicated concentrations of Poly(I:C)-LMW or Poly(A:U) for 6 h. Data are representative (B) or the mean (C, D) of at least three independent experiments. Error bars (C, D) represent SEM. **p* < 0.05, untreated versus Poly(I:C)-treated cells or response of TLR3-WT versus mutant TLR3.



but with significantly reduced efficiency for NF-κB compared with WT TLR3. In contrast, TLR3-Cter₃₅₆-HA was unable to activate either pathway, and TLR3-Cter₃₄₆-HA triggered a weak NF-κB response but no ISRE-dependent response. We next compared the levels of ISRE-dependent transcription in response to increasing concentrations of either LMW Poly(I:C) or Poly(A:U). The dose responses showed that HEK293 cells transfected with WT TLR3 were also significantly more sensitive to LMW Poly(I:C) but not to Poly(A:U) (Fig. 5D). Notably, both C-terminal fragments of the receptor were completely unresponsive to all doses of these two ligands (data not shown). Taken together, these results show that, in agreement with previous reports, uncleaved TLR3 can generate a response to dsRNA (30), whereas the isolated C-terminal fragment triggers only a weak signal (26).

The N- and C-terminal fragments of TLR3 remain associated after cleavage

Because cleaved TLR3 was able to signal in the total absence of TLR3_{FL} (Fig. 4A, 4B, Supplemental Fig. 4A, 4B), whereas isolated TLR3_{C-ter} was almost ineffective (Fig. 5C), we wondered whether the two fragments of TLR3 could remain associated after proteolytic cleavage. Therefore, we compared the profiles of TLR3 on Western blot performed with lysates prepared in nondenaturing (protein lysate neither reduced nor heated) versus denaturing conditions (Fig. 6A–D, Supplemental Fig. 4C). In nondenaturing conditions, we detected the 130 kDa band, whereas

bands corresponding to the proteolytic fragments were barely detectable in epithelial NCI-H292 cells (Fig. 6A, Supplemental Fig. 4C), in mDCs (Fig. 6B), as well as in HEK293-TLR3-HA cells (Fig. 6C, 6D). We ensured that nondenaturing conditions did not prevent the migration of TLR3 fragments, because the constructs corresponding to the cleaved TLR3_{C-ter} fragment (Cter₃₅₆ and Cter₃₄₆) migrated at expected molecular mass (~72 kDa; Fig. 6D). In contrast, when the same lysates were analyzed in denaturing conditions, TLR3_{C-ter} and TLR3_{N-ter} became clearly visible (Fig. 6A–D, Supplemental Fig. 4C), thereby revealing the presence of both uncleaved and cleaved/associated TLR3 in cells. Similarly, when nondenatured lysates were immunoblotted after running on a native gel, the same high molecular band was observed, with HEK293 cells expressing either WT or noncleavable TLR3 and with epithelial cells expressing endogenous TLR3 (Supplemental Fig. 4D). In contrast, the TLR3_{C-ter} mutant migrated on the same gel at a much lower molecular mass. Moreover, nondenaturing conditions showed that Poly(I:C) treatment did not dissociate TLR3_{C-ter} and TLR3_{N-ter} (Fig. 6A–C, Supplemental Fig. 4C). To definitely confirm the association of the two cleaved fragments, we performed immunoprecipitation with C-terminal-specific TLR3.2 and N-terminal-specific TLR3.3 Abs and analyzed the precipitates by immunoblot with the two Abs. In all cases, TLR3_{N-ter} and TLR3_{C-ter} coimmunoprecipitated both in NCI-H292 cells (Fig. 6E) and HEK293-TLR3-HA cells (Fig. 6F). Lastly, reprecipitation after denaturation of the immunoprecipitates ob-

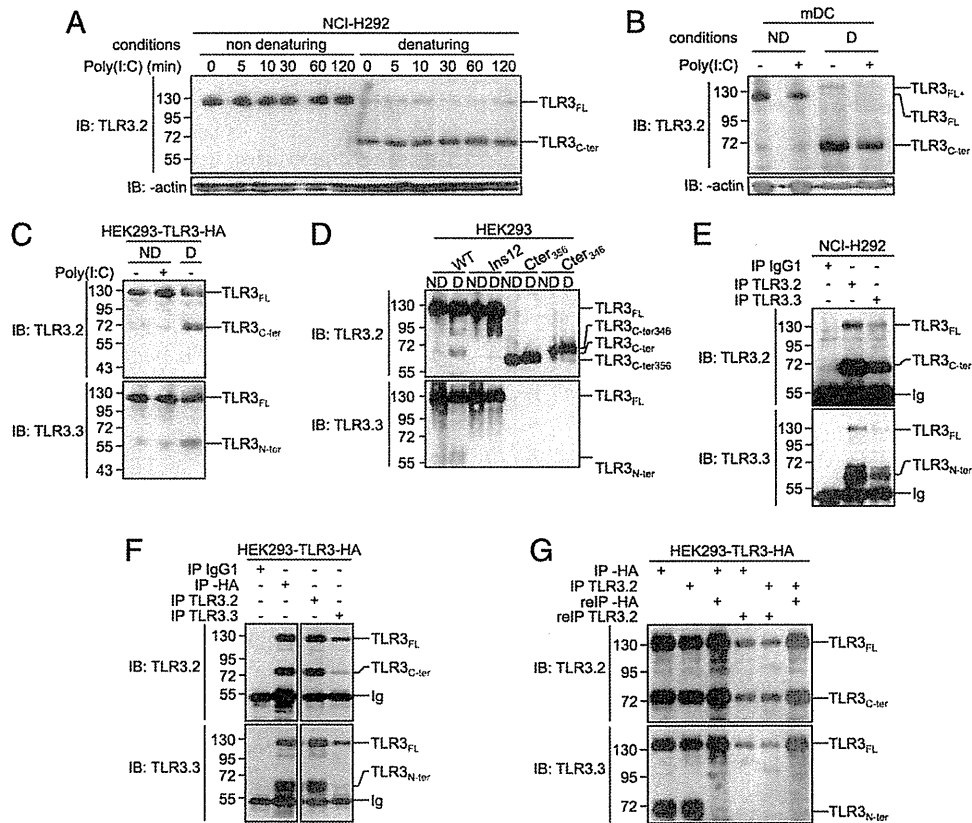


FIGURE 6. The N- and C-terminal fragments of endogenous TLR3 fragments remain associated after cleavage. **(A)** Immunoblot analysis of NCI-H292 cells treated with Poly(I:C) (10 μ g/ml) for the indicated times. Lysates were denatured (D) or not (ND) and then analyzed with TLR3.2 and anti-actin Abs. **(B)** Immunoblot analysis of mDCs treated (+) or not (–) with Poly(I:C) (10 μ g/ml) for the indicated times. Lysates were denatured (D) or not (ND) and then analyzed with TLR3.2 and anti-actin Abs. **(C)** Immunoblot analysis of HEK293-TLR3-HA cells treated (+) or not (–) with Poly(I:C) (10 μ g/ml) for 2 h. Lysates were denatured (D) or not (ND) and then analyzed with TLR3.2 and TLR3.3 Abs. **(D)** Immunoblot analysis of HEK293 cells transfected with TLR3-WT-HA (WT), TLR3-Ins12-HA (Ins12), TLR3-Cter³⁵⁶-HA (Cter³⁵⁶), or TLR3-Cter³⁴⁶-HA (Cter³⁴⁶). Lysates were denatured (D) or not (ND) and then analyzed with TLR3.2 and TLR3.3 Abs. **(E)** Immunoblot analysis of NCI-H292 cells. Lysates were immunoprecipitated with IgG1, TLR3.2, or TLR3.3 Abs and analyzed with TLR3.2 and TLR3.3 Abs. **(F)** Immunoblot analysis of HEK293-TLR3-HA cells. Lysates were immunoprecipitated with IgG1, anti-HA, TLR3.2, or TLR3.3 Abs and analyzed with TLR3.2 and TLR3.3 Abs. **(G)** Immunoblot analysis of HEK293-TLR3-HA cells. Lysates were immunoprecipitated with anti-HA or TLR3.2 Abs and then precipitates were reimmunoprecipitated with anti-HA or TLR3.2 Abs and analyzed with TLR3.2 and TLR3.3 Abs. Values represent molecular mass (kDa). Data are representative of at least three independent experiments.

tained with a C-terminal-specific Ab (either TLR3.2 or anti-HA) led to the loss of the N-terminal fragment of TLR3, confirming that the association of the two fragments was through a noncovalent bond (Fig. 6G). Taken together, our data show that the two fragments of TLR3 remain associated after cleavage and that ligand binding does not disrupt this association (Fig. 7). Therefore, the cleaved/associated TLR3 represents the relevant endogenous TLR3 responsible for the majority of immunological functions.

Discussion

Remarkable progress has been made recently in our understanding of the biology of nucleic acid-sensing TLR3, TLR7, and TLR9. Notably, various data now suggest a model in which exogenous nucleotides can be recognized with high sensitivity, whereas self-nucleotide-induced signaling and autoimmunity are prevented (3). Discrimination between nonself- and self-nucleotides appears to be facilitated by several levels of regulation. Recently, cleavage of TLR9 in endolysosomes was shown to be required for generating the C-terminal fragment of the receptor that binds dsDNA with high affinity and signals. Published data indicated that this mechanism might also apply to TLR3 and TLR7 (9, 22). However, our data allow us to propose an alternative model for TLR3 bi-

ology (Fig. 7), which reconciles two requisites: the need to restrict dsRNA recognition in endolysosomes (and therefore to expose the receptor to a proteolytic environment) to prevent autoreactivity, as described for other endosomal TLRs, and the requirement of the two ligand binding sites present on the ECD of TLR3—the first near the N terminus and the second close to the transmembrane region—to recognize dsRNA with high avidity. Several aspects of the trafficking and processing of TLR3 diverge from what has been described for other lysosomal TLRs (8, 10).

Building on previous observations, and supported by data that were published after the submission of our manuscript (26), our results allow improvement of our model of TLR3 biology. In contrast to TLR9, which was reported to reside principally in the ER in resting cells (32) and to reach the acidic compartments after stimulation by double-stranded DNA (5–7, 33), TLR3 is continuously exported to the Golgi and accumulates in the endolysosomal compartments where it undergoes a single cleavage by cathepsins, most likely within the short (9 aa) LRR12 external loop; however, the exact cleavage site remains unknown. In contrast, asparagine endopeptidase first cleaves the long (30 aa) LRR14–15 flexible loop of TLR9 that is secondarily trimmed by cathepsins (8–10, 34, 35). Strong conservation of the LRR12 ex-

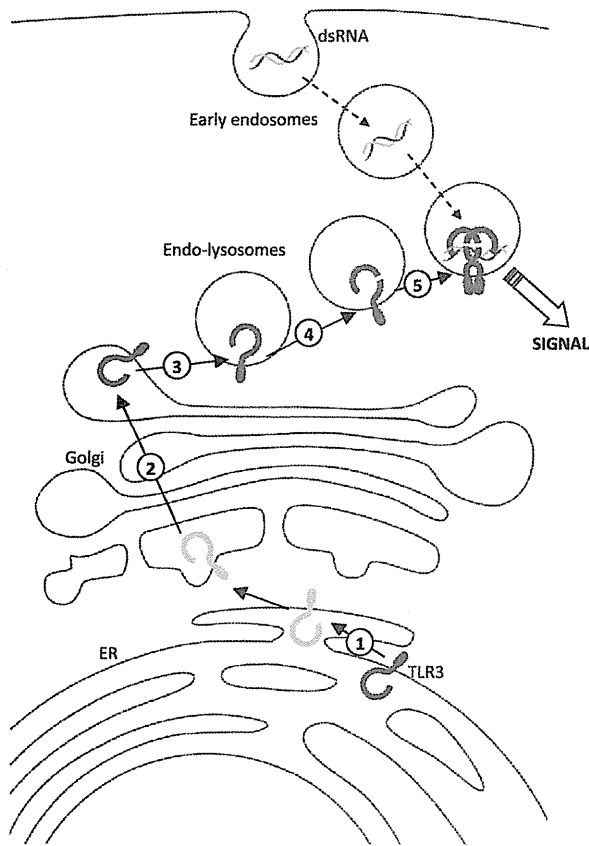


FIGURE 7. Proposed model of TLR3 processing. (1) TLR3 is co-synthesized and *N*-glycosylated in the ER. (2) Then, it crosses the Golgi apparatus where it is fully glycosylated to become EndoH resistant. TLR3 exits the Golgi to enter the endosome membrane (3) where it is cleaved by cathepsins (4). The two proteolytic fragments remain associated to fully signal (5).

ternal loop (residues 335–343) during mammals' evolution (30) suggests that cleavage is an important step in the biology of TLR3. Remarkably, our data confirm that the two proteolytic fragments of the ECD of TLR3 have prolonged half-lives (26) and demonstrate that they remain associated, suggesting that the noncovalent interactions between the adjacent LRRs known to stabilize the ECD of TLRs (36) have been preserved. Furthermore, the absence of detectable amounts of Golgi-modified TLR3_{FL+} in resting immune and nonimmune cells (Figs. 1A, 1D–F, 3B, 3C) indicates that cleaved/associated TLR3 is the almost exclusive form of the receptor present in endolysosomes, where the encounter with exogenous dsRNA is known to occur (37). The lack of appropriate ligand prevented us from visualizing directly TLR3 bound to dsRNA. However, the physical association of TRIF with TLR3_{C-ter}, but not TLR3_{FL+}, after activation with Poly(I:C) in NCI-H292 cells (38), combined with the absence of free TLR3_{C-ter} in those cells, indicates that cleaved/associated TLR3 is the main form of the receptor recognizing Poly(I:C). The single cleavage, without further trimming, may explain why the two long-lived fragments of TLR3 remain associated to bind dsRNA. In contrast, although it was proposed that some TLR9 fragments could remain associated (8, 39), the C-terminal fragment of the receptor is viewed as the major form of the functional receptor, binding agonist CpG oligodesoxynucleotides with high affinity and being able to efficiently recruit the adaptor protein MyD88 (8, 10).

The streamlined transfer to endolysosomes, followed by rapid cleavage, explains why endogenous TLR3 fragments were abundant in resting cells of every type analyzed, whereas TLR3_{FL} was difficult to detect. In contrast, comparable amounts of TLR3_{FL} and TLR3 fragments were observed in HEK293 cells, suggesting an imbalance between the high expression of exogenous TLR3 and the availability of the chaperone protein Unc93b1 in those cells (26). Indeed, exogenous TLR3 was abundant in the endolysosomes. Moreover, the half-lives of the fragments from transfected TLR3 were shorter compared with endogenous TLR3 (compare Fig. 2B with Fig. 2A). These differences should be kept in mind when studying the biology of endosomal TLRs in HEK293 cells.

TLR3 cleavage could increase or decrease the sensitivity of the receptor and/or modify its specificity for different ligands. Our functional studies reveal that, in TLR3-transfected HEK293 cells, the cleavage increased the sensitivity to HMW and LMW Poly(I:C). The increased sensitivity of cleaved/associated TLR3 remains perplexing. Thus, cleavage could somehow increase the affinity of the ECD for its ligands or ease the conformational change that may occur in the presence of dsRNA (39) and that may facilitate the recruitment of TRIF. In agreement with Qi et al. (26), we observed that TLR3_{C-ter} by itself was consistently unable to trigger a strong response to dsRNA. A difference in timing (6 versus 18 h) might explain, in part, the variance between those results and recently published data that showed an equal response to Poly(I:C) with either TLR3-WT or TLR3_{C-ter} (22). Whatever the residual activity of TLR3_{C-ter}, its physiological importance is uncertain, because cleaved/associated TLR3 appears to be the predominant form of the endogenous receptor present in the endolysosomes where recognition of dsRNA takes place.

The central role of cleaved/associated TLR3 highlights the importance for dsRNA binding affinity and sensitive signaling of two distinct ligand-binding sites, each present on one proteolytic fragment. Moreover, the increased sensitivity to Poly(I:C) and the remarkable stability of this form of the receptor allows the reconciliation of some apparently discordant results from the literature. Indeed, one group reported the absence of inhibition of TNF production by RAW macrophages treated for 12 h with cathepsin inhibitors and then for 2 h with 100 µg/ml of Poly(I:C) (8), whereas another group showed a strong suppression of TNF production by the same cells in response to 1 µg/ml of Poly(I:C) (9). These different outcomes may be due to differences in the concentration of ligand used, with high concentrations of dsRNA being able to activate the less efficient TLR3_{FL} in these cells. In addition, our data show that 12 h of Z-FA-fmk pretreatment is not sufficient to suppress the expression of TLR3 fragments in NSCLC cells, suggesting that the lack of inhibition by Z-FA-fmk of cells activated with moderate concentrations of Poly(I:C) could have resulted from the persistence of some cleaved/associated TLR3 at the time of stimulation.

In conclusion, TLR3 provides the first example, to our knowledge, of endosomal receptor maturation by cleavage followed by conversion into a functional cleaved/associated form of the protein. Considering that cleavage of WT-TLR3 is necessary for signaling, cleaved/associated TLR3 is the principal (and possibly exclusive) signaling receptor, and noncleavable TLR3 is able to signal, an intriguing conclusion of the present work is that the licensing consequence of TLR3 cleavage for signaling is not the separation of the two fragments. Further studies are required to fully evaluate the structural and functional consequences of TLR3 processing in vitro and in vivo, as well as to determine to what extent some aspects of TLR3 biology might apply to the other endolysosomal TLRs.

Acknowledgments

We thank Olivier Micheau (Bourgogne University, Dijon, France) for critical reading of the manuscript, Philippe Benaroch for reviewing the results and for the plasmid gift, and Sebastian Amigorena for discussions (both at Curie Institute, Paris, France).

Disclosures

The authors have no financial conflicts of interest.

References

- Kawai, T., and S. Akira. 2011. Toll-like receptors and their crosstalk with other innate receptors in infection and immunity. *Immunity* 34: 637–650.
- Gay, N. J., and M. Gangloff. 2007. Structure and function of Toll receptors and their ligands. *Annu. Rev. Biochem.* 76: 141–165.
- Barton, G. M., and J. C. Kagan. 2009. A cell biological view of Toll-like receptor function: regulation through compartmentalization. *Nat. Rev. Immunol.* 9: 535–542.
- Limmon, G. V., M. Arredouani, K. L. McCann, R. A. Corn Minor, L. Kobzik, and F. Imani. 2008. Scavenger receptor class-A is a novel cell surface receptor for double-stranded RNA. *FASEB J.* 22: 159–167.
- Barton, G. M., J. C. Kagan, and R. Medzhitov. 2006. Intracellular localization of Toll-like receptor 9 prevents recognition of self DNA but facilitates access to viral DNA. *Nat. Immunol.* 7: 49–56.
- Tabeta, K., K. Hoebe, E. M. Janssen, X. Du, P. Georgel, K. Crozat, S. Mudd, N. Mann, S. Sovath, J. Goode, et al. 2006. The Unc93b1 mutation 3d disrupts exogenous antigen presentation and signaling via Toll-like receptors 3, 7 and 9. *Nat. Immunol.* 7: 156–164.
- Kim, Y.-M., M. M. Brinkmann, M.-E. Paquet, and H. L. Ploegh. 2008. UNC93B1 delivers nucleotide-sensing toll-like receptors to endolysosomes. *Nature* 452: 234–238.
- Park, B., M. M. Brinkmann, E. Spooner, C. C. Lee, Y.-M. Kim, and H. L. Ploegh. 2008. Proteolytic cleavage in an endolysosomal compartment is required for activation of Toll-like receptor 9. *Nat. Immunol.* 9: 1407–1414.
- Ewald, S. E., A. Engel, J. Lee, M. Wang, M. Bogyo, and G. M. Barton. 2011. Nucleic acid recognition by Toll-like receptors is coupled to stepwise processing by cathepsins and asparagine endopeptidase. *J. Exp. Med.* 208: 643–651.
- Ewald, S. E., B. L. Lee, L. Lau, K. E. Wickliffe, G.-P. Shi, H. A. Chapman, and G. M. Barton. 2008. The ectodomain of Toll-like receptor 9 is cleaved to generate a functional receptor. *Nature* 456: 658–662.
- Alexopoulou, L., A. C. Holt, R. Medzhitov, and R. A. Flavell. 2001. Recognition of double-stranded RNA and activation of NF-kappaB by Toll-like receptor 3. *Nature* 413: 732–738.
- Casrouge, A., S.-Y. Zhang, C. Eidenschenk, E. Jouanguy, A. Puel, K. Yang, A. Alcais, C. Picard, N. Mahfoufi, N. Nicolas, et al. 2006. Herpes simplex virus encephalitis in human UNC-93B deficiency. *Science* 314: 308–312.
- Zhang, S.-Y., E. Jouanguy, S. Ugolini, A. Smahi, G. Elain, P. Romero, D. Segal, V. Sancho-Shimizu, L. Lorenzo, A. Puel, et al. 2007. TLR3 deficiency in patients with herpes simplex encephalitis. *Science* 317: 1522–1527.
- Guo, Y., M. Audry, M. Ciancanelli, L. Alsina, J. Azevedo, M. Herman, E. Anguiano, V. Sancho-Shimizu, L. Lorenzo, E. Pauwels, et al. 2011. Herpes simplex virus encephalitis in a patient with complete TLR3 deficiency: TLR3 is otherwise redundant in protective immunity. *J. Exp. Med.* 208: 2083–2098.
- Matsumoto, M., H. Oshiumi, and T. Seya. 2011. Antiviral responses induced by the TLR3 pathway. *Rev. Med. Virol.* 21: 67–77.
- Karikó, K., H. Ni, J. Capodici, M. Lamphier, and D. Weissman. 2004. mRNA is an endogenous ligand for Toll-like receptor 3. *J. Biol. Chem.* 279: 12542–12550.
- Wang, Y., L. Liu, D. R. Davies, and D. M. Segal. 2010. Dimerization of Toll-like receptor 3 (TLR3) is required for ligand binding. *J. Biol. Chem.* 285: 36836–36841.
- Bell, J. K., J. Askins, P. R. Hall, D. R. Davies, and D. M. Segal. 2006. The dsRNA binding site of human Toll-like receptor 3. *Proc. Natl. Acad. Sci. USA* 103: 8792–8797.
- Liu, L., I. Botos, Y. Wang, J. N. Leonard, J. Shiloach, D. M. Segal, and D. R. Davies. 2008. Structural basis of toll-like receptor 3 signaling with double-stranded RNA. *Science* 320: 379–381.
- Fukuda, K., T. Tsujita, M. Matsumoto, T. Seya, H. Sakiyama, F. Nishikawa, S. Nishikawa, and T. Hasegawa. 2006. Analysis of the interaction between human TLR3 ectodomain and nucleic acids. *Nucleic Acids Symp. Ser. (Oxf)* 50: 249–250.
- Watanabe, T., T. Tokisue, T. Tsujita, M. Matsumoto, T. Seya, S. Nishikawa, T. Hasegawa, and K. Fukuda. 2007. N-terminal binding site in the human toll-like receptor 3 ectodomain. *Nucleic Acids Symp. Ser. (Oxf)* 51: 405–406.
- Garcia-Cattaneo, A., F. X. Gobert, M. Müller, F. Toscano, M. Flores, A. Lescure, E. Del Nery, and P. Benaroch. 2012. Cleavage of Toll-like receptor 3 by cathepsins B and H is essential for signaling. *Proc. Natl. Acad. Sci. USA* 109: 9053–9058.
- Takada, E., S. Okahira, M. Sasai, K. Funami, T. Seya, and M. Matsumoto. 2007. C-terminal LRRs of human Toll-like receptor 3 control receptor dimerization and signal transmission. *Mol. Immunol.* 44: 3633–3640.
- Sun, J., K. E. Duffy, C. T. Ranjith-Kumar, J. Xiong, R. J. Lamb, J. Santos, H. Masarapu, M. Cunningham, A. Holzenburg, R. T. Sarisky, et al. 2006. Structural and functional analyses of the human Toll-like receptor 3. Role of glycosylation. *J. Biol. Chem.* 281: 11144–11151.
- Kaiser, W. J., J. L. Kaufman, and M. K. Offermann. 2004. IFN- α sensitizes human umbilical vein endothelial cells to apoptosis induced by double-stranded RNA. *J. Immunol.* 172: 1699–1710.
- Qi, R., D. Singh, and C. C. Kao. 2012. Proteolytic processing regulates Toll-like receptor 3 stability and endosomal localization. *J. Biol. Chem.* 287: 32617–32629.
- Chockalingam, A., J. C. Brooks, J. L. Cameron, L. K. Blum, and C. A. Leifer. 2009. TLR9 traffics through the Golgi complex to localize to endolysosomes and respond to CpG DNA. *Immunol. Cell Biol.* 87: 209–217.
- Bell, J. K., I. Botos, P. R. Hall, J. Askins, J. Shiloach, D. M. Segal, and D. R. Davies. 2005. The molecular structure of the Toll-like receptor 3 ligand-binding domain. *Proc. Natl. Acad. Sci. USA* 102: 10976–10980.
- Choe, J., M. S. Kelker, and I. A. Wilson. 2005. Crystal structure of human toll-like receptor 3 (TLR3) ectodomain. *Science* 309: 581–585.
- Ranjith-Kumar, C. T., W. Miller, J. Xiong, W. K. Russell, R. Lamb, J. Santos, K. E. Duffy, L. Cleveland, M. Park, K. Bhardwaj, et al. 2007. Biochemical and functional analyses of the human Toll-like receptor 3 ectodomain. *J. Biol. Chem.* 282: 7668–7678.
- Botos, I., L. Liu, Y. Wang, D. M. Segal, and D. R. Davies. 2009. The toll-like receptor 3:dsRNA signaling complex. *Biochim. Biophys. Acta* 1789: 667–674.
- Leifer, C. A., M. N. Kennedy, A. Mazzoni, C. Lee, M. J. Kruhlak, and D. M. Segal. 2004. TLR9 is localized in the endoplasmic reticulum prior to stimulation. *J. Immunol.* 173: 1179–1183.
- Latz, E., A. Schoenemeyer, A. Visintin, K. A. Fitzgerald, B. G. Monks, C. F. Knetter, E. Lien, N. J. Nilsen, T. Espevik, and D. T. Golenbock. 2004. TLR9 signals after translocating from the ER to CpG DNA in the lysosome. *Nat. Immunol.* 5: 190–198.
- Kasperkovitz, P. V., M. L. Cardenas, and J. M. Vyas. 2010. TLR9 is actively recruited to *Aspergillus fumigatus* phagosomes and requires the N-terminal proteolytic cleavage domain for proper intracellular trafficking. *J. Immunol.* 185: 7614–7622.
- Sepulveda, F. E., S. Maschalidi, R. Colisson, L. Heslop, C. Ghirelli, E. Sakka, A.-M. Lennon-Duménil, S. Amigorena, L. Cabanie, and B. Manoury. 2009. Critical role for asparagine endopeptidase in endocytic Toll-like receptor signaling in dendritic cells. *Immunity* 31: 737–748.
- Manavalan, B., S. Basith, and S. Choi. 2011. Similar structures but different roles – an updated perspective on TLR structures. *Front. Physiol.* 2: 41.
- de Bouteiller, O., E. Merck, U. A. Hasan, S. Hubac, B. Benguigui, G. Trinchieri, E. E. Bates, and C. Caux. 2005. Recognition of double-stranded RNA by human toll-like receptor 3 and downstream receptor signaling requires multimerization and an acidic pH. *J. Biol. Chem.* 280: 38133–38145.
- Estornes, Y., F. Toscano, F. Virard, G. Jacquemin, A. Pierrot, B. Vanbervliet, M. Bonnin, N. Lalaoui, P. Mercier-Gouy, Y. Pachéco, et al. 2012. dsRNA induces apoptosis through an atypical death complex associating TLR3 to caspase-8. *Cell Death Differ.* 19: 1482–1494.
- Li, Y., I. C. Berke, and Y. Modis. 2012. DNA binding to proteolytically activated TLR9 is sequence-independent and enhanced by DNA curvature. *EMBO J.* 31: 919–931.

